Electronic Preprint for Journal of Information Processing Vol.22 No.2

Regular Paper

# Intelligent Resource Scheduling in Green Smart Grid Considering Uncertainties

Shantanu Chakraborty[1,a)] Takayuki Ito[1]

Received: June 28, 2013, Accepted: October 9, 2013

**Abstract:** This paper presents an intelligent economic operation on smart grid environment facilitating an advanced quantum evolutionary method. The proposed method models the wind generation (WG) and the photovoltaic generation (PV) as renewable power generation sources as measures of global warming effect. Thermal generators (TGs) are included in this model to provide the maximum amount of energy to meet consumers' demand. On the other hand, plug-in hybrid electric vehicles (PHEV) are capable of reducing $CO_2$ and gradually becoming an integral part of a smart-grid infrastructure. Such an integration introduces uncertainties into the system that are addressed by a fuzzy agent (FA). The demanded load, the wind speed, the solar radiation and a number of involved PHEVs are taken as fuzzy parameters to resolve uncertainties. An optimizer agent (OA), based on intelligent quantum inspired evolutionary algorithm, is deployed to carry out the economic scheduling operation concerning scheduling and dispatching with the help of FA. OA features intelligent operators such as a sophisticated rotation operator, a differential operator, etc. The method is tested on a hypothetical power system with 10 thermal units, an equivalent number of PHEVs, an equivalent solar and wind farm. The simulation results will show the effectiveness of OA-FA that provides an excellent operational resource scheduling while reducing the production cost and emission.

**Keywords:** smart grid, agent based system, quantum algorithm, unit commitment, renewables, PHEV

## 1. Introduction

Traditional views of power system are reshaping with the concept of smart grid. Economic and environmental incentives, as well as advances in technologies are engineering such a refinement of the electric power industry. Another factor that works for this transformation is the concern regarding the continuous depletion of the finite energy resources such as fossil fuel, natural gas, etc. Moreover, the inevitable environmental changes due to the emission of green house gases such as $CO_2$ have gained the global awareness which is reflected by current rigorous researches oriented on green and clean technologies. Renewable energy sources such as wind and solar energy are thought to be primary sources of alternative energies. On a similar note, Plug-in hybrid electric vehicles (PHEVs) have received increasing interests because of their low pollution emissions and a high fuel economy [1]. The PHEVs will be plugged into the grid, and their onboard energy storage systems will be recharged using clean, renewable energy sources. Therefore, a proper management of PHEVs with renewables and thermal generators is of extreme importance in the future smart grid infrastructure. Strategies regarding the interconnection of PHEV energy storage systems and grids are receiving a great interest in the smart environment since they provide insights of environmental and economical benefits of PHEV. On the environmental point of view, PHEV and TGs will be the main source of emission. Therefore, the intelligent operational strategy should also take the emission into account [2]. Again, the integration of WG and PV with TG and PHEV imposes complications because of the intermittent and fluctuating nature of wind speed and solar radiation. Usually, a stochastic scenario based strategy or fuzzy logic is employed to address such uncertainties. The optimal scheduling as well as the economic load dispatch of TGs is often coined as the Unit Commitment (UC) problem. Hence, UC still remains one of the major operations in a smart grid.

A bibliographical survey on UC reveals that, a good amount of numerical and meta-heuristic optimization techniques such as priority list, the Lagrangian relaxation (LR) [3], [4], the genetic algorithm (GA) [5], [6], the evolutionary programming (EP) [7], the particle swarm optimization (PSO) [8], [9], [10], [26], simulated annealing (SA) [11], [12], dynamic programming (DP) [13] and constraint logic programming (CLP) [15] have been successfully applied to achieve efficient and near optimal solutions for the UC problem. One of the popular set of methods to deal with uncertainties in a nominal UC problem is based on fuzzy logic [14].

Applications of Quantum Mechanics based techniques in the field of operational research of evolutionary methods are considered as a new paradigm [16], [17], [18], [19]. The researches on evolutionary computation coupled with quantum computing trace back to the late '90s. Such efforts can be classified into two categories: i) Quantum algorithms using automatic programming techniques (e.g., genetic algorithm), ii) Quantum inspired evolutionary computation that is crafted based on the principles of quantum mechanics (e.g., uncertainty, superposition, interference, etc.) [20], [21], [22], [23], [24]. Therefore, the applicability

[1] Computer Science and Engineering, Nagoya Institute of Technology, Nagoya, Aichi 466–8555, Japan
[a)] scborty@gmail.com

on quantum evolutionary computing in the field of optimization has already been proven effective.

This paper proposes a Fuzzy Agent (FA) based operational strategy for a smart grid environment powered by thermal generators, solar and wind power and PHEVs. An advanced QA based Optimizer Agent (OA) is applied to perform the economical operation. The method starts with the initialization a group of feasible *solutions* (the OA is responsible for this initiation), which is created by a sophisticated weighted priority list method. A *solution* is comprised of the operating schedules of TGs, their equivalent power dispatches, the solar and wind power dispatch and the number of active PHEVs. The solutions are then 're-observed' and converted into quantum individuals. A FA is then deployed which judges the solutions while taking the load demand, the wind speed, the solar radiation, the spinning reserve, the number of PHEVs and the total production cost into account by imposing fuzzy membership degrees to deal with their associated uncertainties. After judging their corresponding membership values, the control is again given to the OA where the *fitness function* is applied on it to evaluate the level of contribution. The *fitness function* is defined by combining the aggregated fuzzy membership function and the penalty function for constraints violations. For diversifying the individual(s), several operators such as a quantum angle rotation, a GA based mutation and crossover and a new operator based on a binary differential operator are applied.

The rest of the paper is organized as follows. Section 2 presents the basis and underlying mechanism of the applied quantum inspired evolutionary method. The formulations of the proposed model that include the constraints and the objective function are detailed in Section 3. Section 4 describes the fuzzy transformation of uncertain variables by detailing fuzzy membership functions. The key points of OA and FA with operators' specifications are provided in Section 5. Section 6 represents conducted numerical simulations and result analyses. Finally, the conclusion is drawn at Section 7.

## 2. Quantum Computation

The smallest unit of two-state quantum computation is known as quantum bit (hereafter, Q-bit). The Q-bit can take any of these three forms; "1" state, "0" stage or a superposition of these two states. The phenomena is shown in Eq. (1)

$$|\Phi\rangle = \alpha\,|0\rangle + \beta\,|1\rangle \tag{1}$$

where $\alpha$ and $\beta$ are complex numbers that specify the probability amplitudes of the corresponding states. $|\alpha|^2$ and $|\beta|^2$ give the probabilities that whether Q-bit will be located in "0" state and "1" state, respectively. Equation (2) represents the normalization constraints of Q-bit probability amplitudes

$$|\alpha|^2 + |\beta|^2 = 1 \tag{2}$$

Similarly, a *Q-bit individual* is a string of $\lambda$ Q-bits which is defined as

$$\left[\begin{array}{c|c|c|c} \alpha_1 & \alpha_2 & \dots & \alpha_\lambda \\ \beta_1 & \beta_2 & \dots & \beta_\lambda \end{array}\right] \tag{3}$$

where, for each Q-bit, Eq. (2) is satisfied. Q-bit representation is able to present a linear superposition of states and able to represent $2^\lambda$ states in probabilistic manner.

### 2.1 Quantum Individuals in Optimizer Agent (OA)

The lowest level of OA building block corresponds to Q-individuals. As shown in Eq. (3), it contains a number of Q-bits. $Q_i(t)$ denotes the Q-individual $i$ at $t$th generation. Each Q-individual has to be viewed as a distribution of bit strings of length $\lambda$. The fitness of a Q-individual is re-evaluated at every generation according to a realization of distribution even if the individual is unchanged. Which is why, each $Q_i(t)$ is transformed to its binary correspondent, $C_i(t)$ by the process called *collapse* or *observe*. In the context of classical evolutionary algorithms, $Q_i$ is the genotype while $C_i$ is the phenotype. The individual $Q_i$ is further attached to a binary string $A_i$ which acts as an *attractor* for $Q_i$. In every generation, $C_i$ and $A_i$ are compared in terms of both the fitness and bit values. Operators, such as the rotation gate, the bit flipping, the new differential operator, etc. are triggered to the corresponding Q-bit when $A_i$ is better than $C_i$ and their bit values differ. The distribution of $Q_i$ is, therefore, slightly moved toward a given attractor $A_i$. On the other hand, the *attractor* is updated if $C_i$ is better than $A_i$.

### 2.2 Quantum Population

The set of all $n \times m$ Q-individuals forms the *quantum population*. As for Q-groups, the individuals of a Q-population can synchronize their attractors. Therefore, the best attractor (in terms of fitness) among all Q-groups, $B_{global}$, is stored in every generation and is periodically distributed to the group attractors.

### 2.3 Quantum Groups

The population is divided into $m$ Q-groups each containing $n$ Q-individuals having the ability to synchronize their attractors. Therefore, the best attractor of group $k$, $B_{k,g}$ is stored at every generation and is periodically distributed to the group and local attractors.

## 3. Formulation

### 3.1 Thermal Generators

The required fuel cost of generating $P_{i,t}$ power (for the $i$th generator in the $t$th hour) is expressed by the following equation

$$FC_i(P_{i,t}) = a_{0,i} + a_{1,i}.P_{i,t} + a_{2,i}.P_{i,t}^2 \tag{4}$$

where $a_{0,i}$, $a_{1,i}$ and $a_{2,i}$ are the positive fuel cost coefficients for generator $i$. The start-up cost of rebooting a decommitted unit is shown as below

$$SC_i = \begin{cases} hcost_i & : T_i^{\text{off}} \le X_i^{\text{off}} \le H_i^{\text{off}} \\ ccost_i & : X_i^{\text{off}} > H_i^{\text{off}} \end{cases}$$
$$H_i^{\text{off}} = T_i^{\text{off}} + cshour_i. \tag{5}$$

where $T_i^{\text{off}}$ is the minimum down time for generator $i$, while $X_i^{\text{off}}$ is the duration for which generator $i$ is being off. $hcost$ and $ccost$ are the hot and cold start cost for generator $i$, respectively. $cshour$ is the cold start hour of generator $i$. The power output of each generator must be limited within a specified range, i.e.,

$$P_i^{\min} \le P_{i,t} \le P_i^{\max}. \tag{6}$$

where $P_i^{\min/\max}$ are the minimum and maximum operating limit of generator $i$. Again due to operational limitations, once a generator is committed/decommitted it should be kept stable for a minimum period of time before a transition. Such a scenario is covered by the following equation

$$\left.\begin{array}{rcl} T_i^{\text{on}} & \le & X_i^{\text{on}}(t) \\ T_i^{\text{off}} & \le & X_i^{\text{off}}(t) \end{array}\right\}. \tag{7}$$

where $T_i^{\text{on/off}}$ is the minimum up/down time for generator $i$, respectively. $X_i^{\text{on/off}}$ is the duration for which generator $i$ is being ON and OFF, respectively. It is usually assumed for TGs, that the dynamics of a generating plant do not pose restrictions on the amount of power generated at each time period of the time horizon. Unfortunately, this assumption is unrealistic when a smaller time period is involved, since the ramp constraints need to be considered. The following equation (Eq. (8)) addresses this issue

$$sP_i^{\min}(t) \le P_i(t) \le P_i^{\max}(t). \tag{8}$$

where $P_i^{\min}(t) = \max(P_i(t-1) - DR_i, P_i^{\min})$ and $P_i^{\max}(t) = \min(P_i(t-1) + UR_i, P_i^{\max})$. $UR_i$ and $DR_i$ are the up and down ramp limit for unit $i$.

### 3.2 Renewable Sources

The power output from a PV panel depends on the area of the panel, the solar insulation and the efficiency of the panel. The following equation [2] states the PV output in a time period $t$

$$P_{pv,t} = A\mu_{pv}SI_t \tag{9}$$

where $A$ is the PV panel area, $\mu_{pv}$ is the efficiency of the panel and $SI_t$ is the solar insulation at hour $t$. However, determining the wind power is not that straightforward. Due to the complex mechanical nature of a wind turbine, many factors such as the air density, the Albertz Benz constant, the area swept by the turbine rotor etc. The following equation shows the power output

$$P_{wind,t} = (0.5)K\rho_t A(v_t)^3 \tag{10}$$

where $K$ is the Albertz Benz constant, $\rho_t$ is the air density at hour $t$, $A$ is the area, and $v_t$ is the wind speed. Other factors including rated, cut-in and cut out speeds are also considered.

### 3.3 PHEV Battery Model

To gain the maximum benefit from the grid connected PHEVs, they should be operated intelligently and economically. Which is why, the energy price difference, the charging time and the current state-of-charge (SOC) are considered in the proposed model. Such a formulation will allow the PHEVs to join the charging system dynamically. In the case of the peak demand hour, PHEVs are used as a source of energy by discharging the energy stored in their batteries. Again in off-peak demand hour, they can charge up the batteries. In order to operate and determine the contribution of PHEV into the grid, the state-of-charge (SOC) of the installed battery in the PHEV is essential. Therefore, the goal is to maximize the average SOC of all PHEVs. For instance, the remaining $j$th PHEV battery capacity at a particular time $t$ is defined as follows

$$RC_{j,t} = (1 - SOC_{j,t}).C_{\max,j}\alpha \tag{11}$$

where $SOC_{j,t}$ is the current SOC and $C_{max,j}$ is the rated battery capacity of the $j$th PHEV at hour $t$. A weighting function can be defined to control the contribution of factors such as $RC_{j,t}$, the time remaining for charging the $j$th PHEV; $RT_{j,t}$ and the dynamic price difference between the real-time energy price and the price a customer willing to pay for the $j$th PHEV and time $t$; $DP_{j,t}$. Mathematically

$$WF_{i,t} = c_0 RC_{j,t} + c_1 RT_{j,t} + c_2 DP_{j,t} \tag{12}$$

The state-of-charge of the battery for the $j$th PHEVs in $t$th hour ($SOC_{j,t}$) is determined by considering the battery to be a capacitor circuit. $c_{0,1,2}$ are the assigned weights to the associated parameters such that $\sum c_{0,1,2} = 1$. So, the maximization function can be written as

$$\max \sum_{j}^{N_{phev,t}} WF_{j,t}.SOC_{j,(t+1)} \tag{13}$$

where $N_{phev,t}$ is the number of active PHEV in hour $t$. The battery constraint being considered in this paper is the battery output limit, which is defined as

$$SOC_j^{\min} \times P_{phev,j,t} \le P_{phev,j,t} \le SOC_j^{\max} \times P_{phev,j,t} \tag{14}$$

where $P_{phev,j,t}$ is the battery output of $j$th PHEV in $t$th time and $SOC_j^{\min/\max}$ are the range (in percentile) of the battery's SOC. Such constraint will help to keep the battery behavior in sane and longer battery life.

### 3.4 Emission Calculation

Calculating the emission generated from the system is very important from the viewpoint of the environmental aspect. Reducing the emission also factors the success metric of the proposed model. Traditionally, the daily emission from a PHEV is determined by a linear function of emission per mile and the distance covered by that PHEV. Since, the model includes emission, a quadratic function (as stated below; for $NOX$) is defined to determine the $NOX$ emission generation

$$EC_{i,NOX}(P_{i,t}) = \alpha_{0,i} + \alpha_{1,i}.P_{i,t} + \alpha_{2,i}.P_{i,t}^2 \tag{15}$$

where $\alpha_{0,i}$, $\alpha_{1,i}$ and $\alpha_{2,i}$ are the emission coefficients of $NOX$ for generator $i$. The following linear function is applied to generate the $CO_2$ emission

$$EC_{i,CO_2}(P_{i,t}) = \beta_i.P_{i,t} \tag{16}$$

where, $\beta_i$ is the average emission factor for unit $i$. Taking account of the above formulations, the system power balance can be written as (for hour $t$)

$$\sum_{i=1}^{N_{tg}} P_{i,t} + P_{pv,t} + P_{wind,t} \pm \sum_{j=1}^{N_{phev,t}} \mu_{bat} P_{phev,j,t} \times SOC_{j,t} = D_t + Loss \tag{17}$$

($\pm \sum_{j=1}^{N_{phev,t}} \mu_{bat} P_{phev,j} \times SOC_{j,t}$) represents the discharging/charging state of the participating PHEVs batteries, where $\mu_{bat}$ is the PHEV battery efficiency. A sufficient spinning reserve is required in order to maintain the system stability and reliability. The following equation covers that scenario

$$\sum_{i=1}^{N_{tg}} P_{i,t} + P_{pv,t} + P_{wind,t} \pm \sum_{j=1}^{N_{phev,t}} \mu_{bat} P_{phev,j,t} \times SOC_{j,t} \geq D_t + Loss + R_t \quad (18)$$

where $R_t$ is the spinning reserve requirement, which varies from 5% to 10% of the demand depending on the low peak to high peak of load. Finally, the objective function for the optimal economic operation can be stated as

$$\min \sum_{i=1}^{N} \sum_{t=1}^{T} [FC_i(P_{i,t}) + SC_i(1 - I_{i,t-1}) + EC_i] I_{i,t} \quad (19)$$

where the decision variables are $I_{i,t}$ (represents the status of $i$th generator at $t$th hour), $P_{i,t}$ and $N_{phev,t}$. This objective function is subjected to the constraints and conditions that mentioned in this section before.

## 4. Fuzzy Formulation in Fuzzy Agent (FA)

The following subsections describe the fuzzy formulation for non-crisp constraints with associated membership functions.

*Fuzzy load demand:* Since the forecasted load demand is imprecise and can vary with the actual load demand, the crisp notation is transformed by using fuzzy logic onto load demand constraints. Five linguistic values (NE2, NE1, ZE, PE1, PE2) are defined for negative, zero and positive errors. $\mu_{LD}$ is the membership function for the fuzzy load demand.

*Fuzzy spinning reserve:* Spinning reserve ensures the secured and reliable operation during the period of outages. The spinning reserve membership function for the proposed method $\mu_{SR}$ as an exponential function where the higher reserve requirement is encouraged.

*Fuzzy cost function:* The total production cost can also be taken under fuzzy wings by imposing the lower membership function value to a higher production cost schedule. The membership function ($\mu_{TC}$) is a reverse one of that of the spinning reserve.

*Fuzzy solar and wind power:* The solar radiation is a weather variable which again cannot be predicted accurately. Similarly, wind speed can also be unpredictable. Therefore, fuzzy membership functions are defined for those ($\mu_{LR}$ and $\mu_{WR}$, respectively).

*Fuzzy active PHEVs number:* The number of active PHEVs in the grid can also fuzzified using a triangular function with three linguistic variables. The membership degree can be represented as $\mu_{n\_phev}$.

## 5. Agent Functionalities Details

### 5.1 Generating the Initial Solution for Generator's Scheduling

In a trivial QEA algorithm for the mixed integer (MI) problem, the Q-bits are initialized as $[\sqrt{(0.5)}, \sqrt{(0.5)}]^T$ in order to ensure the variables to be equal probable and non-biased to 0/1 state.

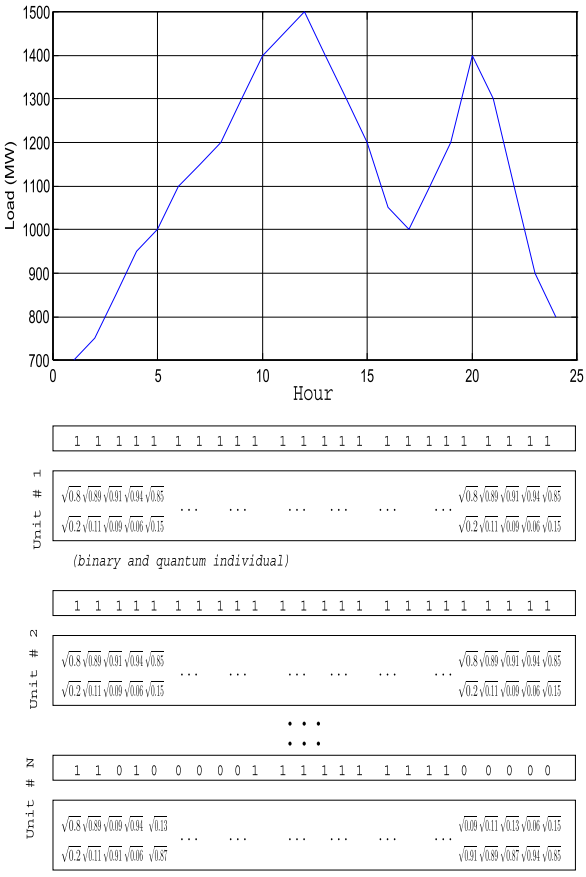


**Fig. 1** Generating initial solution process.

But such an initialization may produce highly infeasible individuals that eventually lead to a slower and premature convergence. In OA, the initialization process for the generator's scheduling problem is accomplished by facilitating a priority list of generators. The process is shown in **Fig. 1**. The generating units are prioritized using a sophisticated weighted priority list method. The units are highly likely to be turned ON in the priority order until the spinning reserve is met for a particular hour. The Q-individual for the corresponding binary individual is set keeping the normalized condition as per Eq. (2).

To satisfy minimum up/down constraints, some excess units are needed to be ON. A logarithmic probability distribution function is used to stochastically set such units.

### 5.2 Strategy for Solving Economic Dispatch (ED) of Committed Units

The committed thermal generator units are provided with a Q-bit where the state superposition represents the weighing factor determining the power output from that unit. Since the Q-bit conveys the information of how much a state is biased to 1 or 0 (refer to Eq. (1), where the complex number $\beta$ represents the probability amplitude of state '1'), the following equation can be defined to generated the units output for a particular population $g$

$$P_{i,t}^{g} = P_i^{\min} + \beta^2 (P_i^{\max} - P_i^{\min}) \quad (20)$$

Such formulation will provide the feasible and quality population since, for the high priority unit, $\beta^2$ is always close to '1' which in turn ensures the higher power output. In every generation, the Q-

bit is updated using some operators, which will be defined in the later section. The lambda iteration method is used to determine the economic load dispatch while taking the initial generation.

### 5.3 Fitness Function

In the proposed method, the fitness function is comprised with the objective function, the penalty function for constraints violation and the aggregated fuzzy membership function that integrates uncertain fuzzy constraints. The aggregated fuzzy membership function for an individual $j$ is defined as

$$\mu_{A_j} = \min(\mu_{LD*}, \mu_{SR*}, \mu_{TC}, \mu_{LR*}, \mu_{WR*}, \mu_{n\_phev}) \tag{21}$$

where

$$\mu_{LD*} = \min(\mu_{LD^1}, \mu_{LD^2}, \ldots, \mu_{LD^T}) \tag{22}$$

$$\mu_{SR*} = \min(\mu_{SR^1}, \mu_{SR^2}, \ldots, \mu_{SR^T}) \tag{23}$$

$$\mu_{LR*} = \min(\mu_{LR^1}, \mu_{LR^2}, \ldots, \mu_{LR^T}) \tag{24}$$

$$\mu_{WR*} = \min(\mu_{WR^1}, \mu_{WR^2}, \ldots, \mu_{WR^T}) \tag{25}$$

The penalty function needs to be defined to measure up the violation index of an individual, which is defined as

$$PF = K.|\_unmet\_demand| + \sum_{k=1}^{ic} C_k |\min(ULD, LLD)| \tag{26}$$

where $K$ is a scaling factor (set as 200). Here $ic$ is the number of inequality constraints, $C_k$ represents the scaling factor associated with related inequality constraints (set as 50). $ULD$ and $LLD$ are the upper and lower limit constraints violations for inequality constraints, respectively. So, the evaluation function is finally defined as

$$E = \frac{10^{round(\log_{10}^{F_{\max}})}}{F + PF} \times \mu_{A_j}. \tag{27}$$

where $F_{\max}$ is a priori value of the maximum fuel cost which is determined by several trials and errors. To normalize the value of $E$ within a scalable range, the numerator is set in accordance with the exponent corresponds to the number of digits in $F_{\max}$. The higher $E$ represents better individual.

### 5.4 Quantum Operators

Several operators such as the rotation gate, the 2-point crossover, the mutation and the differential operator are applied to diversify Q-bits to generate better offsprings. A fuzzy rule is employed to calculate the operators' probabilities to engage. The brief descriptions of the key operators followed by the fuzzy rule are presented below.

#### 5.4.1 Rotation Gate

The rotation gate, $U(\theta)$ is employed on a single Q-bit individual as a variation operator. $(\alpha_{i,j}, \beta_{i,j})$ of the $j$th Q-bit of $i$th individual is updated for the $(t+1)$-th iteration as follows

$$\begin{bmatrix} \alpha_{i,j}(t+1) \\ \beta_{i,j}(t+1) \end{bmatrix} = U(\theta_{i,j}) \begin{bmatrix} \alpha_{i,j}(t) \\ \beta_{i,j}(t) \end{bmatrix} \tag{28}$$

$$= \begin{bmatrix} \cos(\theta_{i,j}) & -\sin(\theta_{i,j}) \\ \sin(\theta_{i,j}) & \cos(\theta_{i,j}) \end{bmatrix} \cdot \begin{bmatrix} \alpha_{i,j}(t) \\ \beta_{i,j}(t) \end{bmatrix}.$$

where the $\theta_{i,j}$ is rotation angle, $\theta_{i,j} = s(\alpha_{i,j}, \beta_{i,j})\Delta\theta_{i,j}$, where $s(\alpha_{i,j}, \beta_{i,j})$ is the sign of $\theta_i$ that determines the direction, $\Delta\theta_{i,j}$ is the magnitude of rotation angle whose lookup table is shown in **Table 1**. The angle $\theta$ is determined based on several trials and errors considering their sensitivity towards the outcome (explained in Section VI). In the table, $B_j$ and $X_j$ represent the $j$th quantum bit of the best solution $B$ and the binary corresponding bit of Q-bit individual, $X$, respectively.

**Table 1** Lookup table for determining the rotation angle for the quantum rotation operation.

| $X_j$ | $B_j$ | $f(r) \geq f(global)$ | $\Delta\theta_j$ | $s(\alpha_j, \beta_j)$ | | | |
|---|---|---|---|---|---|---|---|
| | | | | $\alpha_j\beta_j > 0$ | $\alpha_j\beta_j < 0$ | $\alpha_j = 0$ | $\beta_j = 0$ |
| 0 | 0 | False | 0 | 0 | 0 | 0 | 0 |
| 0 | 0 | True | 0 | 0 | 0 | 0 | 0 |
| 0 | 1 | False | 0 | 0 | 0 | 0 | 0 |
| 0 | 1 | True | $\theta$ | −1 | +1 | ±1 | 0 |
| 1 | 0 | False | $\theta$ | −1 | +1 | ±1 | 0 |
| 1 | 0 | True | $\theta$ | +1 | −1 | 0 | ±1 |
| 1 | 1 | False | $\theta$ | +1 | −1 | 0 | ±1 |
| 1 | 1 | True | $\theta$ | +1 | −1 | 0 | ±1 |

**Table 2** The operators' probabilities determination fuzzy rules table.

| Rule | Antecedent | | | Consequent |
|---|---|---|---|---|
| | $\Delta d$ | $\Delta sr$ | $\Delta tc$ | |
| 1 | NE2 | $sr^*$ | $tc^*$ | VL |
| 2 | NE1 | $sr^*$ | $tc^*$ | L |
| 3 | ZE | $sr^*$ | $tc^*$ | S |
| 4 | PE2 | $sr^*$ | $tc^*$ | L |
| 5 | PE2 | $sr^*$ | $tc^*$ | VL |

#### 5.4.2 Differential Operator

A new differential operator is used in OA to provide diversified Q-bits. The trivial mutation operator does not assure a better offspring. To overcome such a deficiency, the OA uses the information of the best Q-individual in Q-groups. Therefore, the new Q-individual, $Q_{new}(t+1)$ is defined as

$$Q_{new}(t+1) = Q_{r1}(t) + (B_{global}(t) - Q_{r2}(t)) \tag{29}$$

where $Q_{r1}$ and $Q_{r2}$ are two randomly chosen Q-individuals where $r1 \neq r2$, $r1 < r2$ and assuming the Q-individuals are in ascending order according to their fitness, $f(Q_{r1}(t)) < f(Q_{r2}(t))$. Now, the arithmetical operators on the above equation should be transformed to work with Q-individuals or the corresponding *collapsed* binary solutions. Therefore, the above equation is revisited such as follows

$$Q_{new}(t+1) = Q_{r1}(t)\&\&(B_{global}(t)\|Q_{r2}(t))\| (B_{global}(t)\&\&Q_{r2}(t)) \tag{30}$$

### 5.5 Fuzzy Scheme for Operators' Probability in FA

The mentioned operators will not always be applied on individual(s). Rather, in order to reflect the fact that all the individuals are not equally fitted, a fuzzy based rule is undertaken. In order to reduce the disturbance within the high performing individuals, the scheme will apply the operators with the minimum probability while reversing the process for low performance individuals. The fuzzy rules for determining the *engagement probability* to apply on the unary operators are shown in **Table 2**. The corresponding fuzzy membership function for operators' probability is defined as the same triangular function with five linguistic val-

ues. In the case of the *mutation* operator, the *consequent* corresponds to the number of flipping bits instead of the probability itself. The Larsen product is used as the fuzzy implication operator for the individual rules. The union of the results from the fired rules then determines the total output. Finally, the *centroid function* is applied to de-fuzzify the produced output. In case of binary (or more) quantum operators (such as *crossover* and *differential operator*), the engagement probabilities are determined by taking the minimum de-fuzzified crisp output among the engaging individuals.

## 6. Simulation and Result Analyses

The proposed method is applied on a thermal power system of 10 units with an equivalent solar and wind power rating of 40 MW and 25.5 MW, respectively. For simulating, a Pentium IV machine with 2.2 GHz clock speed with 1,024 MB RAM is used. PHP 5.0 and Matlab are used to develop and simulate the program. The generators parameters and load data were reported on reference [3] for 10-units system. Initially, the sensitivity analyses of pivotal parameters are performed.

### 6.1 Sensitivities of Important Parameters in OA

This section presents two analyses of parameters' sensitivities. First, the sensitivity of the rotational angle $\theta$ is scrutinized. Since $\theta$ varies with the nature of applied problem domain [18], it should be chosen carefully. Which is why, several trials are conducted for 10-units system whose results are shown in **Fig. 2**. The figure points out the frequency of hitting the optimal solution range ($563942–$564210) for various values of $\theta$. $\theta$ is varied from 0.005 to 0.05 with step size of 0.0025. It can be seen that, $\theta$ is sensitive. Among the best performing $\theta$-values, 0.03 is chosen. The sensitivity of Q-population size ($G = m \times n$) and a maximum iteration ($MX\_T$) on 10 units system is performed to fix the corresponding parameters. The different trials are shown in **Table 3**. The method is run for 100 times for each of the system configurations. The solution quality of the method is found to be better when ($G$, $MX\_T$):(40, 150). Moreover, the reported standard deviation calculated for this pair is also not significant. The Q-population is divided into 8-groups, each containing 5 Q-individuals.

### 6.2 Thermal Generators with Renewables and PHEV Integration

The number of active PHEV in accordance with the base 10 units power system can be estimated analytically based on the applied region. For this model, a hypothetical region is considered as shown in **Table 4**.

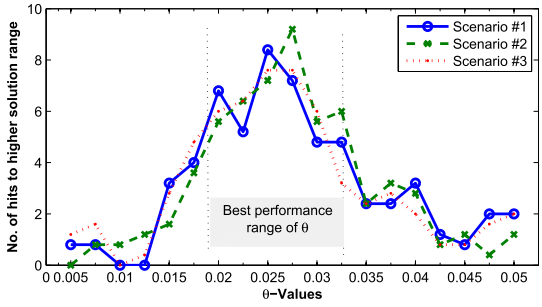


**Fig. 2** Sensitivity of $\theta$ on the performance of OA.

Therefore, according to Ref. [2], the number of PHEVs is roughly 43,000 which is a good estimation of a scenario of an isolated island. Now, a PHEV is estimated to run 32.88 miles/day [24] which tells, that it needs around 8.22 kWh/day. Therefore, the extra energy required for 43K PHEVs is around 353.46 MWh ([43,000 × 8.22]/1,000). An intelligent distribution of such extra power within the thermal generators is required to achieve a certain load leveling.

The highest load demand in 1,500 MW (Hour 12). Usually a typical estimation of the marginal demand which separates the high demand region from the low demand region is 75% of the highest demand. Therefore, 1,125 MW is set as the marginal demand point. According to the demand graph, therefore, Hours (1–6, 16–18 and 22–24) are the off-peak region (total 12 hours). The proposed method intelligently distributes the extra energy required for powering the PHEVs (in this case, 353.46 MW) among these 12 hours. However, instead of equally distributing the required energy, the method uses a different approach. A subroutine is defined which initially sought out the total number of committed units for each of the off-peak hours. According to the priority order of the committed units, the routine then weighs the off-peak hours. The extra required power to support the PHEVs inclusion is distributed according to the defined weights. For instance, **Table 5** shows the weighted hours and corresponding distributions of the extra 353.46 MW. Consequently, the demand curve is modified to reflect these changes.

Therefore, the proposed real-time Quantum Evolutionary Algorithm can dynamically adjust the extra energy within the thermal power. The inclusion of PHEVs will increase demand and

**Table 3** Parameter analysis for 10-units system.

| | $G = 20$ | | | $G = 30$ | | |
|---|---|---|---|---|---|---|
| | $MX\_T$ | | | $MX\_T$ | | |
| | 50 | 75 | 150 | 60 | 100 | 150 |
| Min. | 536,884 | 535,428 | 532,048 | 532,173 | 528,471 | 528,890 |
| Mean | 539,871 | 539,875 | 538,481 | 538,728 | 531,484 | 531,614 |
| Max. | 544,069 | 545,036 | 543,094 | 542,403 | 531,484 | 535,293 |
| Std. dev. | 8.791 | 7.665 | 9.064 | 5.602 | 4.685 | 5.172 |
| | $G = 40$ | | | $G = 50$ | | |
| | $MX\_T$ | | | $MX\_T$ | | |
| | 100 | 150 | 200 | 100 | 150 | 200 |
| Min. | 529,461 | **525,478** | 527,025 | 5,291,048 | 531,584 | 530,247 |
| Mean | 532,238 | **530,734** | 532,746 | 534,197 | 537,044 | 536,310 |
| Max. | 536,109 | **535,807** | 537,048 | 538,991 | 541,879 | 540,094 |
| Std. dev. | 6.074 | **5.358** | 5.914 | 7.725 | 9.815 | 8.223 |

**Table 4** PHEV parameters (Estimated and calculated).

| | |
|---|---|
| PHEV battery capacity | 1,025 kWh |
| Minimum load of the load profile | 700 MW |
| Daily domestic load | 2.08 kW [25] |
| Residential load percentile in the network | 40% |
| Per client PHEV availability | 80% |
| Active participation of residential PHEVs | 40% |

**Table 5** Weighted Priority Hours for load leveling and corresponding extra power requirement (in MW).

| | | | | | |
|---|---|---|---|---|---|
| H:22 | H:18 | H:6 | H:16 | H:5 | H:17 |
| 34.40 | 34.40 | 34.40 | 32.84 | 31.28 | 31.28 |
| H:4 | H:23 | H:3 | H:24 | H:2 | H:1 |
| 29.71 | 28.15 | 26.58 | 25.02 | 23.46 | 21.89 |

**Table 6** Thermal power generation output with smart-grid model (equivalent solar-wind and PHEV storage output) and emission.

| Hour | U 1 | U 2 | U 3 | U 4 | U 5 | U 6 | U 7 | U 8 | U 9 | U 10 | Solar (MW) | Wind (MW) | PHEV (MW) | Power (MW) | Emission (ton) | Cost (USD) |
|---|---|---|---|---|---|---|---|---|---|---|---|---|---|---|---|---|
| 1 | 455 | 150 | 110 | 0 | 0 | 0 | 0 | 0 | 0 | 0 | 0 | 7.2 | −21.96 | 700 | 1,460.9 | 14,582.00 |
| 2 | 455 | 161.8 | 130 | 0 | 0 | 0 | 0 | 0 | 0 | 0 | 0 | 22.27 | −19.09 | 750 | 1,522.5 | 15,128.41 |
| 3 | 455 | 257.1 | 130 | 0 | 0 | 0 | 0 | 0 | 0 | 0 | 0 | 25.5 | −17.93 | 850 | 1,733.7 | 16,785.66 |
| 4 | 455 | 232.6 | 130 | 130 | 0 | 0 | 0 | 0 | 0 | 0 | 0 | 25.5 | −22.65 | 950 | 1,887.2 | 19,219.73 |
| 5 | 455 | 259.6 | 130 | 130 | 25 | 0 | 0 | 0 | 0 | 0 | 0 | 25.5 | −24.98 | 1,000 | 2,006.7 | 20,634.86 |
| 6 | 455 | 352 | 130 | 130 | 25 | 0 | 0 | 0 | 0 | 0 | 0 | 25.5 | −17.52 | 1,100 | 2,267.0 | 22,247.20 |
| 7 | 455 | 399.4 | 130 | 130 | 25 | 0 | 0 | 0 | 0 | 0 | 0.09 | 25.5 | −15.08 | 1,150 | 2,421.2 | 23,076.36 |
| 8 | 455 | 387.7 | 130 | 130 | 25 | 0 | 0 | 0 | 0 | 0 | 17.46 | 25.5 | 29.29 | 1,200 | 2,381.9 | 22,871.57 |
| 9 | 455 | 427 | 130 | 130 | 25 | 20 | 25 | 0 | 0 | 0 | 31.45 | 25.5 | 31.07 | 1,300 | 2,621.3 | 25,556.30 |
| 10 | 455 | 455 | 130 | 130 | 89.6 | 20 | 25 | 0 | 0 | 10 | 36.01 | 25.5 | 23.77 | 1,400 | 2,843.3 | 28,297.39 |
| 11 | 455 | 455 | 130 | 130 | 130.8 | 20 | 25 | 10 | 10 | 0 | 38.06 | 25.5 | 20.56 | 1,450 | 2,946.5 | 30,054.63 |
| 12 | 455 | 454 | 130 | 130 | 120.4 | 20 | 25 | 10 | 10 | 10 | 35.93 | 25.5 | 74.6 | 1,500 | 2,969.7 | 30,769.89 |
| 13 | 455 | 455 | 130 | 130 | 97.6 | 20 | 25 | 0 | 0 | 10 | 36.78 | 25.5 | 15.03 | 1,400 | 2,854.6 | 28,460.95 |
| 14 | 455 | 441.9 | 130 | 130 | 25 | 20 | 25 | 0 | 0 | 0 | 31.59 | 24.82 | 16.76 | 1,300 | 2,675.3 | 25,817.48 |
| 15 | 455 | 414.4 | 130 | 130 | 25 | 0 | 0 | 0 | 0 | 0 | 9.7 | 20.74 | 15.08 | 1,200 | 2,473.0 | 23,339.05 |
| 16 | 455 | 303.8 | 130 | 130 | 25 | 0 | 0 | 0 | 0 | 0 | 12.92 | 14.62 | −21.43 | 1,050 | 2,124.5 | 21,405.47 |
| 17 | 455 | 271.8 | 130 | 130 | 25 | 0 | 0 | 0 | 0 | 0 | 0 | 25.5 | −37.33 | 1,000 | 2,038.0 | 20,847.44 |
| 18 | 455 | 357.2 | 130 | 130 | 25 | 0 | 0 | 0 | 0 | 0 | 0 | 19.04 | −16.22 | 1,100 | 2,283.2 | 22,338.09 |
| 19 | 455 | 372.2 | 130 | 130 | 25 | 20 | 25 | 0 | 0 | 0 | 0 | 25.5 | 17.12 | 1,200 | 2,434.9 | 24,596.87 |
| 20 | 455 | 455 | 130 | 130 | 104.2 | 20 | 25 | 10 | 0 | 0 | 0 | 18.02 | 52.35 | 1,400 | 2,861.4 | 28,567.81 |
| 21 | 455 | 455 | 130 | 130 | 37.4 | 20 | 25 | 0 | 0 | 0 | 0 | 25.5 | 21.98 | 1,300 | 2,736.1 | 26,294.59 |
| 22 | 455 | 358.1 | 128 | 130 | 25 | 0 | 0 | 0 | 0 | 0 | 0 | 21.42 | −17.59 | 1,100 | 2,282.0 | 22,319.60 |
| 23 | 455 | 221.2 | 130 | 130 | 0 | 0 | 0 | 0 | 0 | 0 | 0 | 0 | −36.27 | 900 | 1,860.7 | 19,021.36 |
| 24 | 455 | 150 | 115.7 | 130 | 0 | 0 | 0 | 0 | 0 | 0 | 0 | 2.55 | −52.9 | 800 | 1,684.9 | 17,539.85 |
| | | | | | | | | | | | | | | | $(NO_x + CO_2)$: **55,370.27** | **549,772.54** |

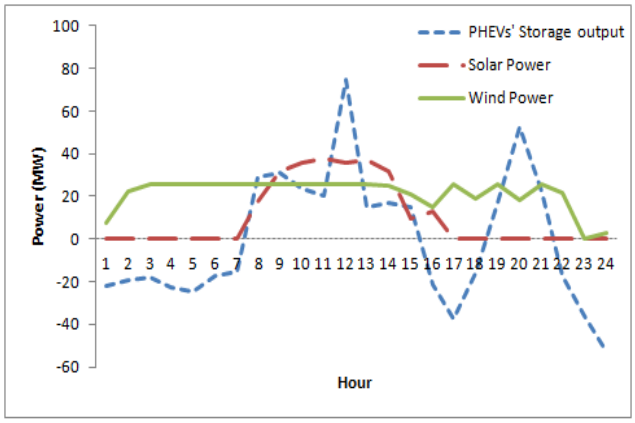


**Fig. 3** The output from renewables and PHEVs' batteries.

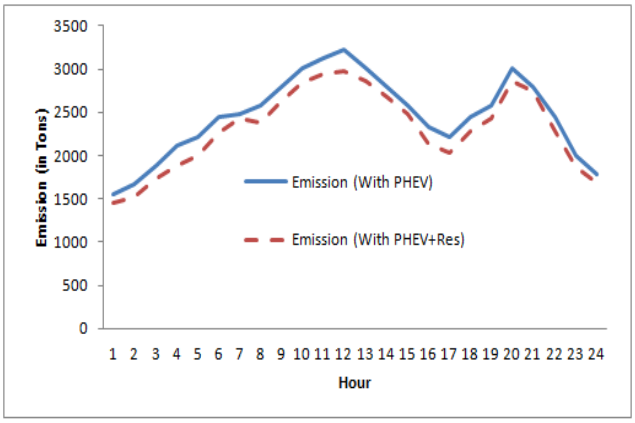


**Fig. 4** Emission reduction in smart-grid model.

emission as well since the thermal units are now responsible for generating extra energies. Therefore, the system requires renewable sources which will nullify such effects. So that brings our next simulation.

The next simulation is conducted by considering the renewable sources (PV and WG) integrated with thermal generators and PHEVs. The rating of the solar farm under study is 40 MW while the wind farm is 25 MW. The economic dispatch of the thermal generators as well as renewable sources and PHEVs' storages are shown in **Table 6**. From that table, it is evident that the proposed model is capable to intelligently schedule and allocate resources. The renewables' power output as well as the aggregated PHEV batteries output are shown in **Fig. 3**. The total emission from thermal generators for that particular case is 55,370.27 tons. This means the inclusion of renewable sources has actually helped to reduce the emission. Accordingly, the production cost is also reduced (down to $549,772.54; note that, the start-up cost is not considered here). The emission reduction phenomena is portrayed in **Fig. 4**.

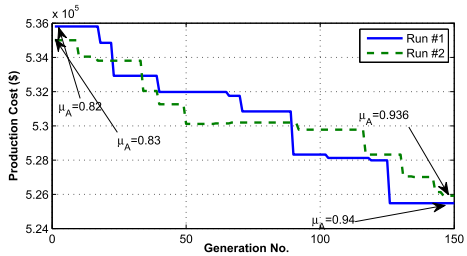


**Fig. 5** Convergence of the proposed method for the 10-units system.

The convergence of OA-FA on a 10-units' system is plotted in **Fig. 5** considering two random cases. The aggregated fuzzy membership function ($\mu_A$) is also pointed in the figure from the starting point of the convergence graph to the settling cost. It can be seen that, the $\mu_A$ is converging as OA-FA reaches to optimality. The fuzzy membership degrees ($\mu_{LD}$, $\mu_{WR}$, $\mu_{SR}$ and $\mu_{LR}$) for different scaled power systems are reported on **Table 7**. The method manages to keep the membership degrees to higher val-

**Table 7** Fuzzy membership degrees for different number units' system.

| Unit | $\mu^*_{LD}$ | $\mu^*_{SR}$ | $\mu^*_{WR}$ | $\mu^*_{LR}$ |
|---|---|---|---|---|
| 10 | 0.9538 | 0.9410 | 0.9363 | 0.9742 |
| 20 | 0.9206 | 0.9177 | 0.9185 | 0.9365 |
| 40 | 0.9152 | 0.9034 | 0.8961 | 0.9241 |
| 60 | 0.9241 | 0.9071 | 0.8828 | 0.8924 |
| 80 | 0.8962 | 0.8875 | 0.8790 | 0.9004 |
| 100 | 0.8634 | 0.8742 | 0.8705 | 0.8593 |

ues that elucidate its capability to generate high quality solutions.

## 7. Conclusion

This paper presents an agent based operational economic strategy for a smart grid with facilitating the fuzzy and optimizer agents (OA-FA). A modified quantum inspired evolutionary algorithm is used as a core of optimizer agent. The purpose of OA-FA is two-fold; 1) to introduce a fuzzy based quantum evolutionary method comprised with several high-performance operators to explore a greater search space by the diversification of solutions, applied on uncertainty based combinatorial optimization problem, and 2) to integrated renewable sources and PHEVs with conventional fuel-based thermal power system to highlight the concern regarding global-warming as well as enhance the research oriented for future smart grid infrastructure. Introducing sophisticated syncing operations between different levels of individuals advances the traditional quantum evolutionary algorithm. Moreover, sophisticated quantum operators are applied for diversifying the individuals that will feature the exploration and exploitation scheme of evolutionary computation. The proposed method intelligently performs the economic operation by reducing the production cost, distributing the renewables and PHEVs charging/discharging scheduling and minimizing the emission. The performed simulation shows the effectiveness of the proposed method. As an evolutionary algorithm, it provides a very smooth convergence graph which ensures its ability to find a balance between local and global search. It can also be safely said that, quantum-based algorithms qualify to be a potential set of solution strategies for the high scaled combinatorial optimization problem. In a more generalized note, the method exhibits to be parallel in nature (considering the fact that although Q-bits are highly coupled, their *entanglement* can be represented as a probability distribution function which helps the manipulation of Q-individuals to be performed in a pseudo-parallel machine), which makes it a potential solution method for the distributed optimization problem. As the simulation results suggest, the proposed algorithm outperforms most of the established methods for the UC problem (both meta-heuristics and mathematical programming). Although, there are no theoretical proofs presented in this paper that explain such result due to the stochastic nature of the algorithm, but analytically speaking, the solution diversification resulted from efficient usage of operators coupled with intelligent generation of initial population have done the trick. Another advantage of such a strategy is upon realising true quantum computers, this class of algorithms will provide very high quality solutions with a minimum amount of computational effort (with a O(1) complexity).

## References


[1] Moreno, J., Ortúzar, M.E. and Dixon, J.W.: Energy-management system for a hybrid electric vehicle, using ultra capacitors and neural networks, *IEEE Trans. Ind. Electron.*, Vol.53, No.2, pp.614–623 (Apr. 2006).

[2] Saber, A.Y. and Venayagamoorthy, G.K.: Efficient Utilization of Renewable Energy Sources in by Gridable Vehicles in Cyber-Phyical Energy Systems, *IEEE System Journal*, Vol.4, No.3, pp.285–294 (2010).

[3] Ongsakul, W. and Petcharaks, N.: Unit commitment by enhanced adaptive Lagrangian relaxation, *IEEE Trans. Power Syst.*, Vol.19, No.1, pp.620–628 (Feb. 2004).

[4] Peterson, W.L. and Brammer, S.R.: A capacity based Lagrangian relaxation unit commitment with ramp rate constraints, *IEEE Trans. Power Syst.*, Vol.10, No.2, pp.1077–1088 (May 1995).

[5] Kazarlis, S.A., Bakirtzis, A.G. and Petridis, V.: A genetic algorithm solution to the unit commitment problem, *IEEE Trans. Power Syst.*, Vol.11, No.1, pp.83–92 (Feb. 1996).

[6] Senjyu, T., Yamashiro, H., Uezato, K. and Funabashi, T.: A unit commitment problem by using genetic algorithm based on unit characteristic classification, *Proc. 2002 IEEE Power Eng. Soc. Winter Meeting*, Vol.1, pp.58–63 (2002).

[7] Juste, K.A., Kita, H., Tanaka, E. and Hasegawa, J.: An evolutionary programming solution to the unit commitment problem, *IEEE Trans. Power Syst.*, Vol.14, No.1, pp.1452–1459 (Nov. 1999).

[8] Ting, T.O., Rao, M.V.C. and Loo, C.K.: A Novel approach for unit commitment problem via an effective hybrid particle swarm optimization, *IEEE Trans. Power Syst.*, Vol.21, No.1, pp.411–418 (Feb. 2006).

[9] Chakraborty, S., Senjyu, T., Saber, A.Y., Yona, A. and Funabashi, T.: Optimal thermal unit commitment integrated with renewable energy sources using advanced particle swarm optimization, *IEEJ Trans. Electrical and Electronics Eng.*, Vol.4, No.5, pp.609–617 (Sep. 2009).

[10] Chakraborty, S., Ito, T., Senjyu, T. and Saber, A.Y.: Unit Commitment Strategy of Thermal Generators by Using Advanced Fuzzy Controlled Binary Particle Swarm Optimization Algorithm, *International Journal of Electrical Power & Energy Systems*, Vol.43, No.1, pp.1072–1080 (Dec. 2012).

[11] Simopoulos, D.N., Kavatza, S.D. and Vournas, C.D.: Unit commitment by an enhanced simulated annealing algorithm, *IEEE Trans. Power Syst.*, Vol.21, No.1, pp.68–76 (Feb. 2006).

[12] Zhuang, F. and Galiana, F.D.: Unit commitment by simulated annealing, *IEEE Trans. Power Syst.*, Vol.5, No.1, pp.311–318 (Feb. 1990).

[13] Ouyang, Z. and Shahidehpour, S.M.: An intelligent dynamic programming for unit commitment application, *IEEE Trans. Power Syst.*, Vol.6, No.3, pp.1203–1209 (Aug. 1991).

[14] El-Saadawi, M.M., Tantawi, M.A. and Tawfik, E.: A fuzzy optimization based approach to large scale thermal unit commitment, *Electr. Power Syst. Res.*, Vol.72, pp.245–252 (2004).

[15] Huang, K.Y., Yang, H.T. and Huang, C.L.: A new thermal unit commitment approach using constraint logic programming, *IEEE Trans. Power Syst.*, Vol.13, No.3, pp.936–945 (Aug. 1998).

[16] Moore, M. and Narayanan, A.: *Quantum-Inspired Computing*, Dept. of Compute. Sc., University Exter, Exterm U.K. (1995).

[17] Narayanan, A. and Moore, M.: Quantum-inspired genetic algorithm, *Proc. IEEE Int. Conf. Evolutionary Computation*, Japan, pp.61–66 (1996).

[18] Spector, L., Barunum, H., Bernstien, H.J. and Swamy, N.: Finding a better-than-classical quantum AND/OR algorithm using genetic programming, *Proc. 1999 Congr. Evolutionary Computation*, Piscataway, NJ, Vol.3, pp.2239–2246, IEEE Press (July 1999).

[19] Han, K.H. and Kim, J.H.: Quantum-inspired evolutionary algorithm for a class of combinatorial optimization, *IEEE Trans. Evol. Compute.*, Vol.6, No.6, pp.580–593 (Feb. 2006).

[20] Babu, G.S.S., Das, D.B. and Patvardhan, C.: Real parameter quantum evolutionary algorithm for economic load dispatch, *IET Gen. Trans. Dist.*, Vol.2, No.1, pp.22–31 (Nov. 2008).

[21] Lau, T.W., Chung, C.Y., Wong, K.P., Chung, T.S. and Ho, S.L.: Quantum-inspired evolutionary algorithm approach for unit commitment, *IET Gen. Trans. Dist.*, Vol.2, No.1, pp.22–31 (Nov. 2008).

[22] Chung, C.Y., Yu, H. and Wong, K.P.: An advanced quantum-inspired evolutionary algorithm for unit commitment, *IEEE Trans. Power Syst.*, paper accepted for publication, DOP: Aug. 2010.

[23] Jeong, Y., Park, J., Jang, S. and Lee, K.Y.: A new quantum-inspired binary PSO: Application to unit commitment problems for power systems, *IEEE Trans. Power Syst.*, Vol.25, No.3, pp.1486–1495 (Aug. 2010).

[24] Coelho, L.S.: Gaussian quantum-behaved particle swarm optimization approaches for constrained engineering design problems, *Expert Systems with Applications*, Vol.37, pp.1676–1683 (2010).

[25] Roe, C., Meliopoulos, A.P., Meisel, J. and Overbye, T.: Power system level impacts of plug-in hybrid electric vehicles using simulation data,

*Proc. IEEE Energy 2030*, Atlanta, GA (Nov. 2008).
[26] Chakraborty, S., Senjyu, T., Yona, A., Saber, A.Y. and Funabashi, T.: Solving economic load dispatch problem with valve-point effects using a hybrid quantum mechanics inspired particle swarm optimisation, *Generation, Transmission & Distribution*, Vol.5, No.10, pp.1042–1052, IET (2011).

**Shantanu Chakraborty** is currently working as an Assistant Manager in Smart Energy Laboratory in NEC Corporation in Japan. Prior to join NEC, he was positioned as a Research Assistant Professor in Nagoya Institute of Technology, Nagoya, Japan from April, 2012 to August, 2013. He doctored in March, 2012 in Interdisciplinary Intelligent System Engineering (majoring in Power System Economic) from University of the Ryukyus, Japan under PESC Laboratory funded by Monbukagakusho (MEXT). While conducting Ph.D. research, worked as a Research and Teaching Assistant. Finished Masters in Engineering from University of the Ryukyus in 2009 majoring in Electrical and Electronics Engineering. His research interests include Smart Grid, Distributed System, Multi-agent System, Optimization Strategies, Operational research, etc. He is an active member of IEEE and IEEJ.

**Takayuki Ito** is an Associate Professor of Nagoya Institute of Technology. He received his B.E., M.E, and Doctor of Engineering from Nagoya Institute of Technology in 1995, 1997, and 2000, respectively. From 1999 to 2001, he was a Research Fellow of the Japan Society for the Promotion of Science (JSPS). From 2000 to 2001, he was a Visiting Researcher at USC/ISI (University of Southern California/Information Sciences Institute). From April 2001 to March 2003, he was an Associate Professor of Japan Advanced Institute of Science and Technology (JAIST). From 2005 to 2006, he is a Visiting Researcher at Division of Engineering and Applied Science, Harvard University and a Visiting Researcher at the Center for Coordination Science, MIT Sloan School of Management. From 2008 to 2010, he was a Visiting Researcher at the Center for Collective Intelligence, MIT Sloan School of Management. He is a board member of IFAAMAS, the PC-chair of AAMAS2013, PRIMA2009, General-Chair of PRIMA2014, and was a SPC/PC member in many top-level conferences (IJCAI, AAMAS, ECAI, AAAI, etc). He received the JSPS Prize, 2014, the Prize for Science and Technology (Research Category), the Commendation for Science and Technology by the Minister of Education, Culture, Sports, Science, and Technology, 2013, the Young Scientists' Prize, the Commendation for Science and Technology by the Minister of Education, Culture, Sports, Science, and Technology, 2007, the Nagao Special Research Award of the Information Processing Society of Japan, 2007, the Best Paper Award of AAMAS2006, the 2005 Best Paper Award from Japan Society for Software Science and Technology, the Best Paper Award in the 66th Annual Conference of 66th Information Processing Society of Japan, and the Super Creator Award of 2004 IPA Exploratory Software Creation Projects. He is Principle Investigator of the Japan Cabinet Funding Program for Next Generation World-Leading Researchers (NEXT Program). Further, he has several companies, which are handling web-based systems and enterprise distributed systems. His main research interests include multi-agent systems, intelligent agents, group decision support systems, agent-mediated electronic commerce, and software engineering on offshoring.